

# Design and Characterization of a Compact Single Layer Modified S-Shaped Tag Antenna for UHF-RFID Applications

**Mohammed Ali Ennasar<sup>1</sup>, Ikram Aznabet<sup>2</sup>, Otman El Mrabet<sup>2</sup>, Mohamed Essaaidi<sup>1,2</sup>**

<sup>1</sup>Smart systems laboratory (SSL), Higher School of IT (ENSIAS), Mohamed V University, Rabat, Morocco

<sup>2</sup>Information and Telecommunication Systems Laboratory (LaSiT), Faculty of Sciences, Abdelmalek Essaadi University, Tetuan, Morocco

\*corresponding author, E-mail: o.mrabet@gmail.com

## Abstract

In this paper, we report the design of a new compact single layer modified S-shaped tag antenna for UHF-RFID applications. To achieve a compact size of  $51 \times 34 \text{ mm}^2$  for this tag antenna, the technique of using S shaped strip is applied, and by further adding a pair of equilateral triangular stubs into this structure, good impedance matching can be obtained at 915 MHz, which is the center frequency of the North-American UHF-RFID band (902 to 928 MHz). Besides exhibiting acceptable 5m read range in free space at 915 MHz, the proposed design shows a read range of about 4.5 when mounted on a metallic object ( $200 \times 30 \text{ cm}^2$ ) separated by spacer foam of thickness 1 cm. Furthermore, the proposed design shows a reasonable read ranges when it is mounted on different dielectrics with low permittivity. The proposed design has a simple configuration, low cost, acceptable read range, and can work on various background materials.

## 1. Introduction.

Radio frequency identification is a rapidly developing technology that uses electromagnetic waves to automatically identify or track people and objects. Recently, it has been extensively used in inventory control and management, logistics operations, bio engineering, manufacturing and retail, etc. [1-2]. RFID system throughout the world operates in low frequency (LF, 125 KHz), high frequency (HF, 13.56 MHz), ultra-high frequency (UHF, 860-960 MHz) and microwave frequency (MW, 2.45 GHz, 5.8 GHz) bands. In the last years, ultra-high frequency (UHF) radio-frequency identification (RFID) technology has gained much attention owing to its longer read-range and higher data transfer rate [3] as compared to the low-frequency (LF) and high-frequency (HF) bands.

In terms of design procedure for UHF RFID systems, the input impedance of the tag antenna must be conjugate matched with that of the RFID chip impedance to achieve maximum power transfer [4]. In most cases dipole type antennas were adopted and designed for UHF-RFID applications [5] owing to their omnidirectional behavior.

However, RFID tag antennas must be compact, light, and easy to fabricate for mass production. Furthermore, depending on specific application, RFID tag antennas are mountable on different materials (metal, dielectrics...), which can affect seriously their performance. Therefore, there is a need for the design of RFID tag antennas for general RFID applications. So far, various types of RFID tag antennas have been reported in the literature [6-12]. For example in [6] the authors provide only the read range of the RFID tag antenna mounted on paper reel. In [7], C. Chi et al. developed a new RFID tag antenna in free space with a high read range achieved by inserting some CP radiation elements. In contrast, the authors in [8] study the effect of different materials on the reading range of the RFID tag antenna. Different RFID tag antennas in UHF band have been proposed in literature operating on metallic objects [9], liquid solutions [10-11] and for on body applications [12]. However, most of the proposed tag antennas are suitable for a specific application which could limit their versatility.

This situation has motivated us to overcome this problem. Thus, in this paper, a new compact RFID-UHF modified S-shaped antenna which can be mounted on different materials is proposed. To provide a good conjugate matching between the S-shaped antenna and the chip, the technique of adding asymmetrical triangular stubs on both sides of the tag chip was applied. This technique enables to keep the compact size of the antenna as well as to easily match the RFID chip impedance and the antenna impedance. Furthermore, the proposed S-shaped tag antenna is single layer and can be easily printed on cheap substrates, which make the final design low cost and low profile. A commercial simulator, CST Microwave Studio has been used to explore the main characteristics of the proposed RFID tag antenna.

## 2. RFID tag antenna design and equivalent circuit model

The physical structure of this proposed design is simple and consists of two meandered strips that have the form of S-shaped structure, connected in the middle by a chip, see Figure 1. To keep the antenna size compact and to get a

good matching with the chip, both meandered strips are loaded with an equilateral triangular stub. All the strips are coated on a FR4 substrate with thickness  $h=1.58$  mm, relative permittivity  $\epsilon_r = 4.4$ , and loss tangent  $\tan \delta = 0.025$ . The top antenna trace was made of copper having a thickness of  $35 \mu\text{m}$ . The total area of the proposed structure is  $51 \times 43 \text{ mm}^2$ , which corresponds to  $(0.155 \lambda_0 \times 0.13 \lambda_0)$ , where  $\lambda_0$  is the free-space wavelength at 915 MHz.

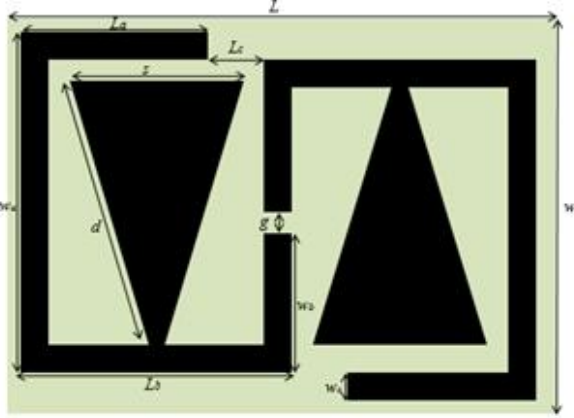


Figure 1: Structural configuration of the proposed RFID Tag antenna.

The proposed S-shaped modified tag antenna is designed to operate in the RFID-UHF band of 902–928 MHz (North American Band). Murata LXMS31ACNA chip with an impedance of  $Z_{\text{Chip}} = (17.6-j100.9)$  at 915 MHz is selected for our design. The minimum threshold power to activate this chip is -8 dBm. Note that the impedance of the chip was measured using the same technique described in [13] which is a little different from the one ( $Z_{\text{Chip}} = 12-j107$ ) reported in the datasheet [14]. This discrepancy can be attributed to the accuracy of the method that we have used here to evaluate the input impedance of the chip is different from the one used by the manufacturer. The input impedance of the antenna has to be  $(17.6+j100.9)$  to achieve a maximum power transfer. The final optimized geometrical parameters obtained by using CST Microwave studio are listed in Table. 1.

TABLE I  
Dimensions of RFID tag antenna [mm]

L	L <sub>a</sub>	L <sub>b</sub>	L <sub>c</sub>	w <sub>a</sub>	w <sub>b</sub>	w <sub>c</sub>	w	d	g	s
51	15.6	26	7.4	36	15.5	3	43	30	2	18

The RFID chip used in this work exhibits a high capacitive reactance ( $Z_{\text{Chip}} = 12-j107$ ), to cancel the latter the technique of adding asymmetrical triangular stubs on both sides of the tag chip is introduced. In this case, the triangular stubs can be regarded as a short transmission line that is analogous to an inductive reactance connected in series to the tag, which in turn increase the inductive reactance of the antenna. Therefore, optimizing the parameters of the

triangular stubs (d and s) appropriately can provide a good conjugate matching. To verify this conjecture, we have simulated the reflection coefficient of the proposed RFID tag antenna with and without the triangular stubs. The obtained results are presented in Figure. 2.

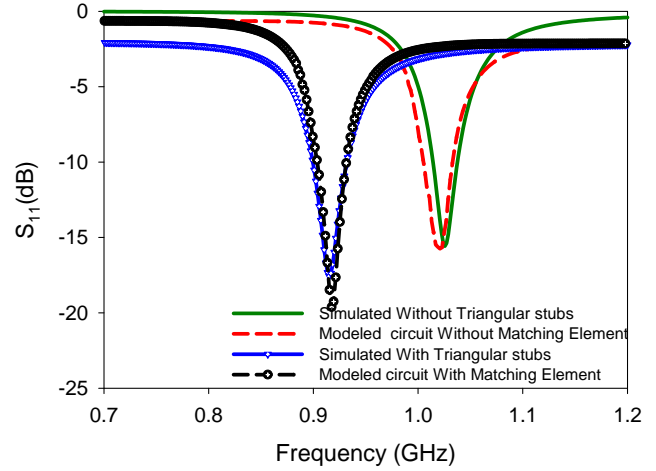


Figure 2: Modeled and simulated reflection coefficient of the proposed RFID tag antenna with and without the triangular stubs.

One can see easily that without triangular stubs, a resonant frequency appears at 1.01 GHz. However, with the triangular stubs this resonant frequency shifts down to 915 MHz. This result reveals that the introduction of triangular stubs into the proposed structure has equivalent effect of increasing the electrical length of the antenna while keeping the same total size of the proposed design. Thus, we can conclude that the triangular stubs act as an inductor. To further explain the operating principle of the reactive matching of the proposed design, we have simulated the current distribution of the structure with and without the triangular stubs at 915 MHz which are displayed in Figure. 3. It can be clearly seen that adding triangular stubs increases the electrical length of the proposed structure, resulting in larger inductance effect in the structure.

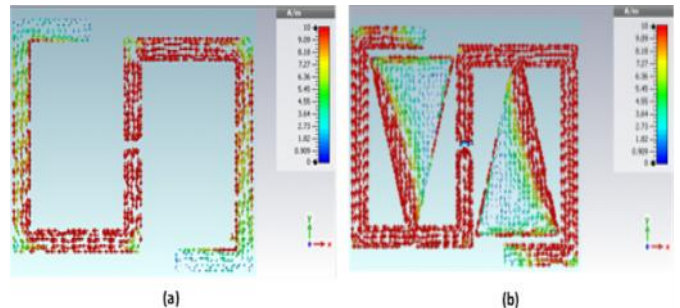


Figure 3: Simulated distributed current of the proposed structure with and without the triangular stubs at the resonance frequency.

Moreover, the reflection coefficient of the RFID tag antenna

was modelled using a lumped elements circuit as shown in Figure. 4. For the sake of simplicity, the RFID chip and the antenna can be modelled as a series RC ( $R_{chip}$ ,  $C_{chip}$ ) and a series RLC circuit ( $R_{ant}$ ,  $L_{ant}$ ,  $C_{ant}$ ), respectively. The lumped elements values have been obtained by using approximate equations, especially for the antenna. For example, according to [15], the radiation resistance for a small dipole can be approximated by

$$R_a = 80f^2r^2\left(\frac{l}{w}\right) \quad (1)$$

where  $0.5 \leq \alpha \leq 1$  depending on how the current is distributed along the antenna, and  $l$  is the length of the antenna. By considering the working frequency of the antenna at 1.01 GHz, the radiation resistance is supposed to be  $R_{ant}=15.9 \Omega$  when  $\alpha$  is equal to 0.6 and the length of the antenna is 93 mm. To find the inductance of the antenna, we can use the approximated formula given in [16]:

$$L_{ant} = \frac{\mu_0}{2f} l \left( \ln\left(\frac{l}{w}\right) + \frac{f}{2} \right) \quad (2)$$

where  $l$  and  $w$  are respectively the length and width of the conductive strip. The antenna capacitance can be obtained by using the self-resonant frequency of the proposed antenna  $f_c = \frac{1}{2f\sqrt{L_{ant}C_{ant}}}$  where  $L_{ant}$  and  $C_{ant}$  are the

equivalent inductance and capacitance of the antenna structure respectively. Therefore the capacitance is given by

$$C_{ant} \approx \frac{1}{4f^2L_{ant}} \quad (3)$$

The value of  $L_{ant}$  is then found to be 25.6 nH. From Eqs.1, 2 and 3 we have approximate values for a series RLC circuit model of the proposed antenna. The equivalent circuit for MURATA RFID chip is a 17.6  $\Omega$  resistor in series with a 1.64 pF capacitor. The two triangular stubs used as matching network can be modelled as a series inductance ( $L_{series}$ ). To demonstrate the validity of this lumped circuit model, the reflection coefficient  $S_{11}$ (dB) obtained by using a circuit simulator (Agilent's Advanced Design System) is compared with the 3D full wave simulation as shown in Figure 2. The modelled results are in good agreement with the simulated data, confirming that the proposed equivalent circuit model is acceptable and accurate.

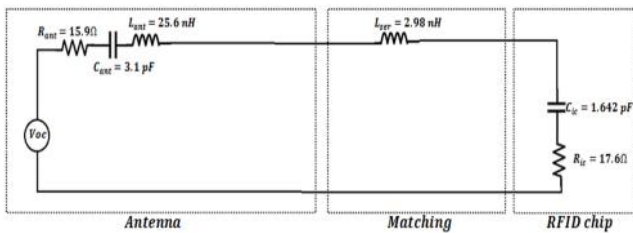


Figure 4: Equivalent circuit model of the proposed RFID tag antenna.

The slight different between circuit model and 3D full wave results, especially after and before the resonance, can be ascribed to the fact that the circuit model proposed here is a simplified circuit model which allows an easy design of the proposed RFID tag antenna near to the operating frequency band and doesn't take into account the behavior of the structure outside the operating band.

### 3. Measurements results and discussion

To verify the above results, a prototype of the proposed RFID tag antenna has been fabricated and measured. The reflection coefficient and input impedance of the proposed RFID tag antenna was measured using a Rohde & Schwarz ZVB 20 Network analyzer through a differential probe as shown in Figure.5.

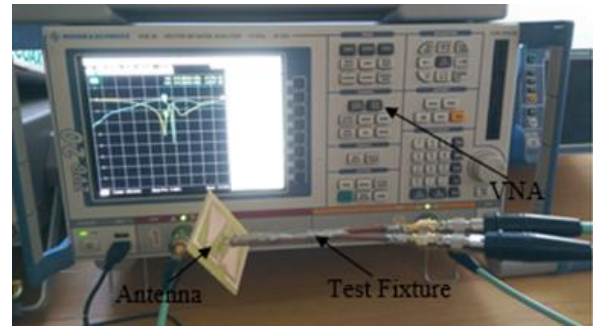


Figure 5: Measurement setup using Rohde & Schwarz ZVB 20 VNA with test fixture soldered to the antenna

The antenna reflection coefficient is then extracted from the measured S-parameters over the frequency band of interest using the same method reported in [17]. Figure.6 shows the measured and simulated reflection coefficient of the RFID tag antenna. There is a good agreement between the measured and simulated results. The measured -10dB bandwidth is ranging from 900 MHz to 928 MHz for a total bandwidth of 28 MHz and is centered at 0.914 MHz, which can cover totally the North-American UHF RFID band.

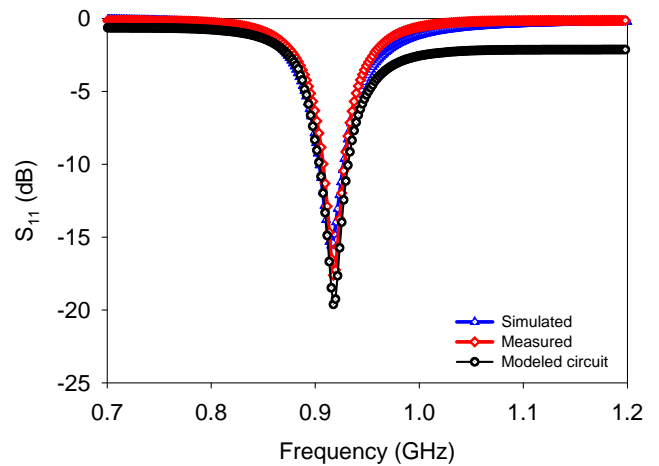
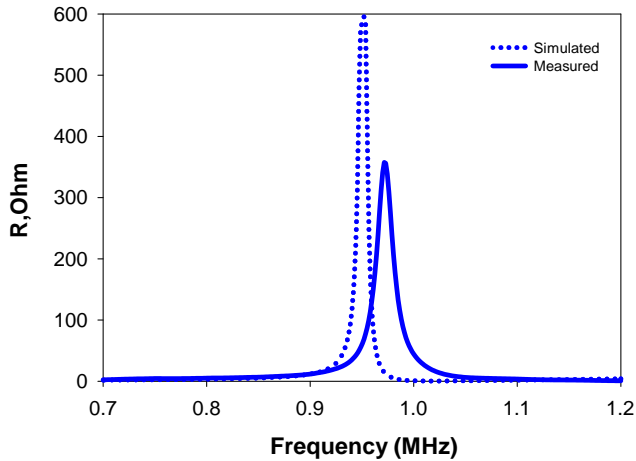
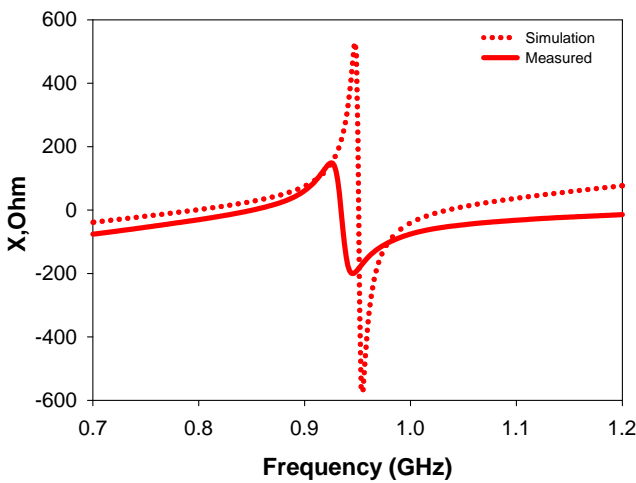


Figure 6: Reflection coefficient of  $S_{11}$  calculated from the simulated, the equivalent circuit model, and the measured impedance

Figure. 7 shows the measured and simulated input impedances of the prototype in free space. From measurement, the impedance of the antenna is approximately  $(16.43+j112.3 )$  at 915MHz, which is very close to the measured conjugate impedance of the used chip  $(17.6-j100.9 )$ .



(a)



(b)

Figure 7: Measured and simulated input impedances of the prototype RFID tag antenna, (a) Resistance, (b) Reactance.

The tag sensitivity of the (Minimum power activation) of the proposed design was also investigated using the backscatter measurement setup depicted in Figure.8. This system consists of two horn antennas, a digital oscilloscope (Agilent DSO91204A), a pulse generator (Picosecond Pulse Labs Model 3500). The whole system is controlled by homemade software based on Matlab. The transmitter and the receiver horn antennas (SAS-571) have very large bandwidth (700 MHz up to 18 GHz) and provide a flat 13 dBi gain over the frequency range from 860 to 960 MHz. One horn antenna collects the backscatter signal produced

by the tag and a digital oscilloscope (Agilent Infiniium) is connected to the other horn antenna and allows the measurement of the tag power activation. In this setup, the horn antenna is placed 0.42 m away from the RFID tag antenna. It is worthwhile to note that the measurements were performed in an anechoic chamber, as shown in Figure. 9, at LCIS lab, Valence, France. The minimum power activation is presented in Figure. 9. It can be clearly seen that the measured minimum power to activate the tag at 915 MHz is -7 dBm. Next, we have measured the read range, which is considered as the main parameter that characterize an RFID system.

From the measured results of the activation power presented in Figure.9 (a), the read range of the RFID tag antenna can be determined using the following formula [4]:

$$r_{\max} = d \sqrt{\frac{P_{EIRP}}{G_t P_{th}}} \quad (4)$$

where  $d$  is the distance between the RFID tag antenna and the transmitter antenna of the measurement system.  $P_{th}$  is the minimum transmitted power obtained from the measurement system to activate the tag,  $G_t$  is the gain of Transmitting antenna, and  $PEIRP$  is the maximum output allowed transmitted power.

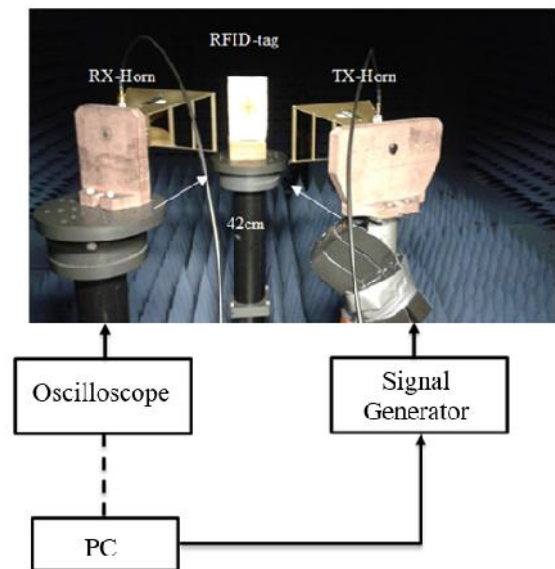


Figure 8: Power activation measurement setup

The measured read range versus the frequency over the 902-928 MHz band is presented in Figure.9 (b) for  $EIRP = 4W$ . The results reveal that within the operation bandwidth (902-928 MHz) the read range is above 4.5 m, confirming that the proposed structure is capable to operate at North-American band with a good performance. At 915 MHz, the maximum read range was found to be 5.25 m in free space which is very close the calculated one. This value of the read range indicates that a good conjugate matching between the antenna and the RFID tag is obtained. It is worth noting that

when compared to the read range of the RFID tags reported in [18], the proposed design has higher read range value.

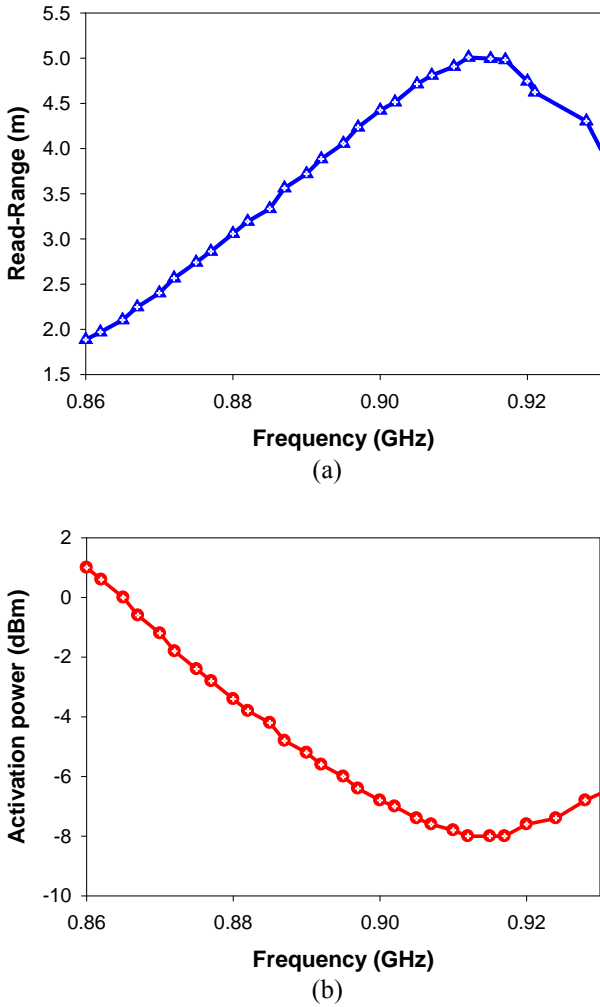


Figure 9: Activation power and Read range as a function of frequency: (a) Measured activation power, (b) Measured and simulated read range.

In the above paragraph, we have measured the read range in free space, however, in the real world, RFID tags antennas are often mounted on different materials (e.g., Glass, Metal, liquid, plastic, wood, cardboard...). In this situation, the antenna properties such as radiation pattern, impedance and radiation efficiency may be drastically affected especially in UHF band. Thus, we have measured the read range of the proposed design mounted on different materials in an ordinary room as shown in Figure 10. The measurement setup used here is similar to the one reported in [19] and include Thing Magic Micro (M6e-M) UHF RFID development kit [20], stepper motor (Brother model KE58KM2-032), a driving board and a single circularly polarized patch antenna having a gain of 6 dBi at the frequency range of 800-1000 MHz. The RFID reader is connected to the antenna via 1.8 m of 50 coaxial cable model CNT-195-FR to generate 36 dBm at 915 MHz. Hence, the total transmitted power was approximately 4W

EIRP (effective isotropic radiated power). The RFID tag antenna attached on a foam substrate was oriented in the line of sight direction of the RFID reader, as shown in Figure. 10. Both of them are kept fixed and the distance separation between them is 0.5m. Note that the measurements of the read range of the proposed structure mounted on different objects were carried out at our laboratory (LaSiT, Morocco) using the formula given in [19]. The obtained results are presented in Figure. 11. It can be observed that the RFID tag antenna has an acceptable read range when it is mounted on glass, plastic, wood, and cardboard. For the case where the tag antenna is mounted on a 1 cm thin foam spacer for use on a metallic object, the maximum read range was found to be 4.52 m. We have also investigated the effect of the foam spacer thickness on the read range. For foam spacer of 2 mm, 6 mm, and 8 mm thickness, the obtained read range was found to be 0.5 m, 2 m, and 4 m, respectively. These obtained results showed that the read range decreased with decreasing thickness of the foam layer.

This is owing to the fact that proposed structure was designed and optimized without a ground plane which can deteriorate drastically the performance of the RFID tag antenna. Note that, here we have used a low-cost foam dielectric (polyethylene) which is attractive owing to its easy integration into the roll-to-roll process. Therefore, the proposed design is suitable to be installed in a recessed cavity in metallic objects such as vehicles, and metallic containers. It is worthwhile to mention that the proposed structure can demonstrate farther read ranges on different objects because of the RFID chip used in this paper has  $P_{th} = -8$  dBm and this value is certainly very high if compared to other chips like NXP G2XL, and Alien Higgs. For example, if an NXP G2XL IC chip with  $P_{th} = -17$  dBm is used in the design of this RFID tag antenna the calculated read range would be 12.43 m.



Figure 10: RFID tag read range measurement setup in real conditions.

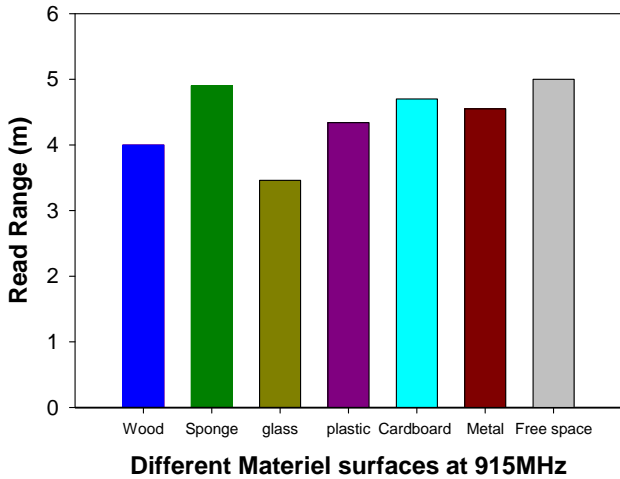


Figure 11: Measured Read range of the proposed RFID tag antenna mounted on different materials in real conditions

Finally, we have measured the 2-D reading patterns of the RFID tag antenna in the (x-y) and (y-z) planes at 915 MHz by using the same measurement set-up described above. The reading range patterns of the proposed structure were measured in an ordinary room. To measure the read range pattern at the operation frequency of 915 MHz in the x-y and y-z planes, the RFID tag antenna was rotated from 0° to 360° stepped by 10°. Here, we have used a stepper motor (Brother Model KE58KM2-032) with 4 GPIO ports and minimum angular step of 1.8° to rotate the rotating platform. The connection between the stepper motor and the RFID reader is realized using Arduino Mega 2560 as shown in Figure 10. The obtained results are presented in Figure 12 which shows that the reading pattern is omnidirectional radiation pattern in the y-z plane with the maximum read range of 5 m. However, the reading pattern in the x-y plane reveals that the maximum read range has decreased to 3.8 m and the pattern is quite close to a more directional one.

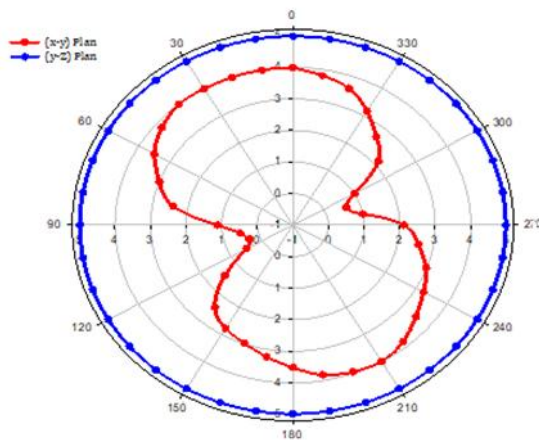


Figure 12: Measured read range patterns of the proposed RFID tag

For both planes, slight variation (0.3 m) of the read range is

observed specially between back and front read ranges. Additionally, it is found that the maximum read range in the x-y plane is tilted by 15° which is may be caused in particular by the effect of the surface current distribution concentrated around the triangular stubs.

#### 4. Conclusions

A compact modified S-shaped tag antenna for UHF-RFID applications is studied numerically and experimentally. The antenna is one single layer and designed using a low-cost substrate (FR4) with a total size of  $51 \times 43 \times 16 \text{ mm}^3$ . Two triangular stubs are used to achieve conjugate matching for the desired input resistance and reactance. The measured 10-dB impedance bandwidth of the proposed design is 28 MHz which covers the entire 902-928 MHz band designed for North America. The maximum read range measured in free space was found to be 5.2 m. The experimental results show also that the proposed design can have a maximum read range of 4.2 m when separated by a 1 cm thin foam spacer from a large metallic plate ( $200 \times 30 \text{ cm}^2$ ). In addition, the experimental results reveal that the proposed design has demonstrated acceptable read range when mounted on different materials which make it suitable for general UHF-RFID applications, except for liquid bottles.

#### Acknowledgements

This work was supported by the Moroccan Ministry of Higher Education. (MESRSFC) and the CNRST under grant number PPR2/2015/36. The assistance of Prof. Smail Tedjini, Laboratoire de Conception et d'Intégration des Systèmes, Grenoble-INP, Valence 26902, France, in the various experiments is noted and appreciated.

#### References

- [1] K. Finkenzeller, RFID Handbook: 'Radio-Frequency Identification Fundamentals and Applications', 2nd ed. New York, NY, USA: Wiley, 2004.
- [2] L. Jeremy, 'The history of RFID' IEEE Potentials, vol. 24, no. 4, pp. 8–11, Oct.–Nov. 2005.
- [3] S.-H. Jeong and H.-W. Son, 'UHF RFID tag antenna for embedded use in a concrete floor' IEEE Antennas Wireless Propag. Lett. vol. 10, , 2011 pp. 1158–1161.
- [4] P. V. Nikitin, K. V. S. Rao, S. F. Lam, V. Pillai, R. Martinez, and H. Heinrich, 'Power reflection coefficient analysis for complex impedances in RFID tag design' IEEE Trans. Microw. Theory Tech., vol. 53, no. 9, pp. 2721–2725, Sep. 2005.
- [5] N.C. Karmakar, Handbook of smart antennas for RFID systems. John Wiley & Sons. Hoboken, New Jersey, 2010.
- [6] L. Ukkonen, Ang Yu, L. Sydanheimo, Fan Yang, M. Kivikoski and A. Elsherbeni, 'Analysis of bow tie array RFID tag antenna for paper reel identification systems,' 2007 IEEE Antennas and Propagation Society

- International Symposium, Honolulu, HI, 2007, pp. 2745-2748.
- [7] C. Cho, I. Park, and H. Choo, 'Design of a circularly polarized tag antenna for increased reading range', *IEEE Trans Antennas Propag* 57 (2009), 3418–3422.
- [8] T. Deleruyelle, P. Pannier, M. Egels and E. Bergeret, "An RFID Tag Antenna Tolerant to Mounting on Materials," in *IEEE Antennas and Propagation Magazine*, vol. 52, no. 4, pp. 14-19, Aug. 2010.
- [9] H.D. Chen, S.H. Kuo, C.Y.D. Sim, and C.H. Tsai, "Coupling-feed circularly polarized RFID tag antenna mountable on metallic surface", *IEEE Trans Antennas Propag* 60 (2012), 2166–2174.
- [10] R. Quiroz, T. Alves, B. Poussot and J. M. Laheurte, "Combined RFID tag antenna for recipients containing liquids," in *Electronics Letters*, vol. 49, no. 4, pp. 240-242, Feb. 14, 2013.
- [11] R. Gonçalves, R. Magueta, P. Pinho and N. B. Carvalho, "RFID passive tag antenna for cork bottle stopper," *IEEE Antennas and Propagation Society International Symposium (APSURSI)*, Memphis, TN, 2014, pp. 1518-1519, 2014.
- [12] M. M. Tentzeris et al., "Inkjet-printed RFID-enabled sensors on paper for IoT and "Smart Skin" applications," *ICECom 2013*, Dubrovnik, 2013, pp. 1-4.
- [13] M. Daiki, H. Chaabane, E. Perret, S. Tedjni, T. Aguil, "RFID Chip Impedance Measurement for UHF Tag Design, " *Progress in Electromagnetics Research Symposium (PIERS'11)*, Mar 2011, pp.679, 2011.
- [14] <http://www.murata.com/~media/webrenewal/support/library/catalog/products/k70e.ashx>
- [15] D. B. Miron, *Small Antenna Design*, Burlington, MA, USA: Newnes, 2006.
- [16] F. E. Terman, *Radio Engineer's Handbook*. New York: McGraw-Hill, 1945.
- [17] X. Qing, C. K. Goh and Z. N. Chen, "Impedance Characterization of RFID Tag Antennas and Application in Tag Co Design," in *IEEE Transactions on Microwave Theory and Techniques*, vol. 57, no. 5, pp. 1268-1274, May 2009.
- [18] C. Cho, H. Choo and I. Park, "Broadband RFID tag antenna with quasi-isotropic radiation pattern," in *Electronics Letters*, vol. 41, no. 20, pp. 1091-1092, 29 Sept. 2005.
- [19] R. Colella, L. Catarinucci, P. Coppola, and L. Tarricone "Measurement Platform for Electromagnetic Characterization and Performance Evaluation of UHF RFID Tags", *IEEE Trans Antennas Propag* 65 (2016), 905-914.
- [20] ThingMagic M6e Hardware Guide, [online] Available: <http://www.thingmagic.com> , Sep. 2017.